

Field-Temperature Phase Diagram and Entropy Landscape of CeAuSb₂

Lishan Zhao,^{1,2} Edward A. Yelland,^{1,3} Jan A. N. Bruin,^{1,4} Ilya Sheikin,⁵ Paul C. Canfield,⁶ Veronika Fritsch,^{7,8} Hideaki Sakai,^{1,9} Andrew P. Mackenzie,^{1,2} and Clifford W. Hicks²

¹*Scottish Universities Physics Alliance (SUPA), School of Physics and Astronomy, University of St. Andrews, St. Andrews KY16 9SS, United Kingdom*

²*Max Planck Institute for Chemical Physics of Solids, Nöthnitzer Str. 40, 01187 Dresden, Germany*

³*SUPA, School of Physics and Astronomy, and Centre for Science at Extreme Conditions, University of Edinburgh, Mayfield Road, Edinburgh EH9 3JZ, United Kingdom*

⁴*Max Planck Institute for Solid State Research, Heisenbergstr. 1, 70569 Stuttgart, Germany*

⁵*Laboratoire National des Champs Magnétiques Intenses (LNCMI-EMFL), CNRS, UJF, F-38042 Grenoble, France*

⁶*Ames Laboratory and Department of Physics, Iowa State University, Ames, Iowa 50011, U.S.A.*

⁷*Experimental Physics VI, Center for Electronic Correlations and Magnetism, Institute of Physics, University of Augsburg, 86135 Augsburg, Germany*

⁸*Physikalisches Institut, Karlsruhe Institute of Technology, 76131 Karlsruhe, Germany*

⁹*Department of Physics, Osaka University, Toyonaka, Osaka 560-0043, Japan*

(Dated: 17 Feb 2016)

We report a field-temperature phase diagram and an entropy map for the heavy fermion compound CeAuSb₂. CeAuSb₂ orders antiferromagnetically below $T_N = 6.6$ K, and has two metamagnetic transitions, at 2.8 and 5.6 T. The locations of the critical endpoints of the metamagnetic transitions, which may play a strong role in the putative quantum criticality of CeAuSb₂ and related compounds, are identified. The entropy map reveals an apparent entropy balance with Fermi liquid behavior, implying that above the Néel transition the Ce moments are incorporated into the Fermi liquid. High-field data showing that the magnetic behavior is remarkably anisotropic are also reported.

PACS numbers:

Introduction

CeAuSb₂ is a heavy-fermion system with the tetragonal $P4/nmm$ structure, moderate electrical anisotropy, and strong magnetic anisotropy. [1] Although it has not been widely studied, it shows strong phenomenological similarities with other cerium-based compounds that have received intense interest. A major theme of study of Ce-based systems is to understand and tune the balance between Kondo and RKKY interaction: RKKY interaction couples localized spins and favors a magnetically ordered ground state, while strong Kondo interaction quenches local spins, incorporating their entropy into the Fermi liquid. Data presented in this paper, and comparison with other compounds, suggest that CeAuSb₂ is on the border, with the effects of both Kondo and RKKY interactions apparent in its bulk properties, but neither dominating.

A field-temperature phase diagram of CeAuSb₂ is shown in Fig. 1; the indicated phase boundaries are from this work, however many of its basic features were published in Refs. [2] and [3]. At zero field, there is a Néel transition at $T_N = 6.6$ K. As the field is increased, there are two first-order metamagnetic transitions, at 2.8 and 5.6 T. The magnetic order terminates at the second metamagnetic transition.

There appear to be many materials with qualitatively similar field-temperature phase diagrams, including CeNiGe₃, [4, 5] CeRh₂Si₂, [6, 7] and YbNiSi₃, [8, 9] and the CeRu₂Si₂-based compounds

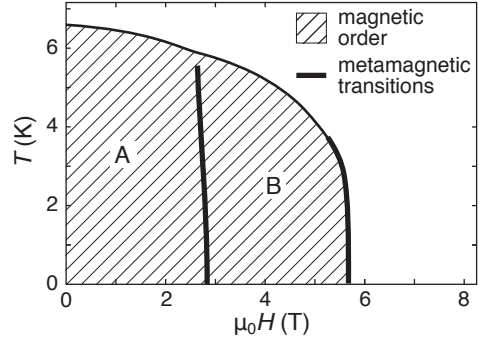


FIG. 1: Field-temperature phase diagram of CeAuSb₂, with the magnetically ordered region and the metamagnetic transitions shown. The indicated phase boundaries are from this work.

(Ce_{0.8}La_{0.2})Ru₂Si₂, [10–12] CeRu₂(Si_{0.9}Ge_{0.1})₂, [13, 14] and Ce(Ru_{0.092}Rh_{0.08})₂Si₂. [15, 16] All of these compounds show antiferromagnetism and, when the field is oriented along the easy axis, two metamagnetic transitions. With the exception of Ce(Ru_{0.92}Rh_{0.08})₂Si₂, the magnetic order of each terminates at the second metamagnetic transition.

At low temperatures, all of the Ce-based compounds listed above have strongly anisotropic easy-axis magnetic susceptibilities. χ_c/χ_a of CeAuSb₂ is 17 just above T_N . [1] χ_c/χ_a of CeRh₂Si₂ is 5 just above its Néel temperature, and of CeRu₂Si₂, 15 at 10 K. [17, 18] CeNiGe₃

is an orthorhombic system where the a axis is the easy axis; χ_a/χ_b and χ_a/χ_c are 11 and 17, respectively, just above its T_N . [4]

Therefore, study of CeAuSb₂ is likely to have bearing on a range of other compounds. Comparison with the CeRu₂Si₂-based compounds is of particular interest. CeRu₂Si₂ itself has a Kondo temperature T_K of ~ 24 K, [18] and strong antiferromagnetic fluctuations at low temperature, but no static order; [19] the Kondo effect appears to win out over the RKKY interaction by a small margin. Substitution can alter the balance: partial substitution of La for Ce, *e.g.* decreases T_K and induces the static antiferromagnetic order mentioned above. [12, 20, 21] The substitution applies an effective negative pressure: the lattice is expanded, and when it is compressed again with (positive) hydrostatic pressure the antiferromagnetism is suppressed. [22] The similarity between the phase diagrams of CeAuSb₂ and substituted CeRu₂Si₂-based compounds suggests that CeAuSb₂ acts, broadly, as a negative-pressure version of CeRu₂Si₂. Usefully, it is a version without intrinsic substitution disorder or, with reference to Ce_{1-x}La_xRu₂Si₂, dilution of Ce spins. It may allow RKKY-Kondo crossover to be studied with positive rather than negative pressure.

The main aim of the present work is to refine the phase diagram of CeAuSb₂. The metamagnetic transitions are thought to be first-order, but clear hysteresis has not been seen and their critical endpoints have not been precisely located. [2] As will be elaborated upon in the Discussion, the endpoints may prove crucial to possible quantum criticality in CeAuSb₂, and related compounds. In addition to locating the critical endpoints of CeAuSb₂, we also report an entropy map across the field-temperature phase diagram, which yields both similarities and notable contrasts with the above compounds.

Crystal growth

Single CeAuSb₂ crystals were grown by a self-flux method, similar to that described in Refs. [23] and [24]. High purity ingots of Ce (99.99%, Ames Laboratory), Au (99.999%, Alfa Aesar), and Sb (99.999%, Alfa Aesar) were placed in an alumina crucible with a Ce:Au:Sb atomic ratio of 1:6:12. The crucible was then sealed in an evacuated quartz ampoule and heated to 1100°C for 10 hours, followed by cooling to 700° over a period of 100 hours. The excess flux was decanted with a centrifuge at 700°C. Measurement by energy-dispersive X-ray spectroscopy (EDX) confirmed that the crystals are stoichiometric to within the 5% measurement precision. The residual resistivity ratios of the crystals used in this work were between 6 and 9. A photograph of an as-grown CeAuSb₂ crystal is shown in Fig. 2.

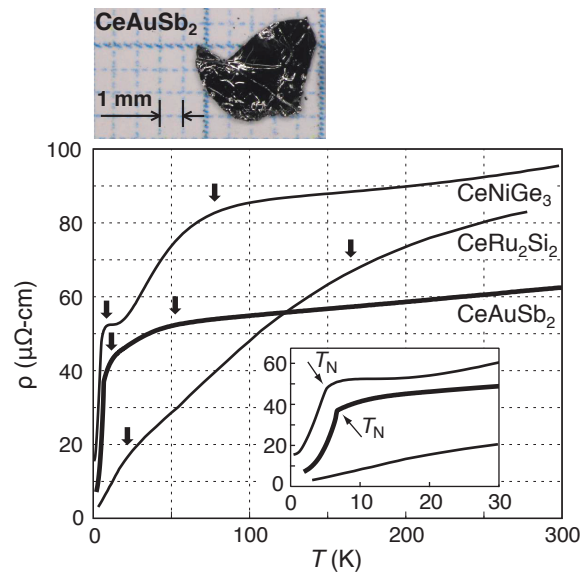


FIG. 2: Top: a photograph of an as-grown crystal of CeAuSb₂. Bottom: comparison of $\rho(T)$ of CeNiGe₃ (Ref. [4]), CeRu₂Si₂ (Ref. [18]), and CeAuSb₂ (this work). For CeRu₂Si₂ and CeAuSb₂, the current \mathbf{I} is in the plane, and for CeNiGe₃, an orthorhombic material, $\mathbf{I} \parallel \hat{c}$. The arrows mark broad shoulders, discussed in the text.

Results: resistivity

For measurement of resistivity, samples were cut into narrow bars with a wire saw. The as-grown samples were naturally thin along the c axis, so polishing to reduce thickness was not necessary. The samples were measured with a typical four-terminal method using a lock-in amplifier, with typically a 100 μ A excitation current at a frequency on the order of 100 Hz. Contacts to the sample were made with DuPont 6838 silver paste, baked at 180° C for 2.5 hours.

We start in Fig. 2 with a comparison of the resistivities $\rho(T)$ of CeAuSb₂, CeRu₂Si₂, and CeNiGe₃. The room-temperature values are similar; respective comparison of CeAuSb₂ with LaAuSb₂ [25] and CeRu₂Si₂ with LaRu₂Si₂ [18] show that scattering from cerium spins accounts for roughly half the resistivity at room-temperature, and a greater portion as T is reduced. The resistivities also all show two broad shoulders, marked by the arrows in Fig. 2. The higher-temperature shoulders are due to thermal occupation of excited crystal electric field states. The origin of the lower-temperature shoulders may differ from compound to compound; in CeRu₂Si₂ it is attributed to the Kondo effect. [18] In both CeNiGe₃ and CeAuSb₂ the shoulder is at a lower temperature than in CeRu₂Si₂; both these compounds also show Néel order, so the lower-temperature shoulder could be due to onset of short-range magnetic order at $T > T_N$, or the Kondo effect, or a combination.

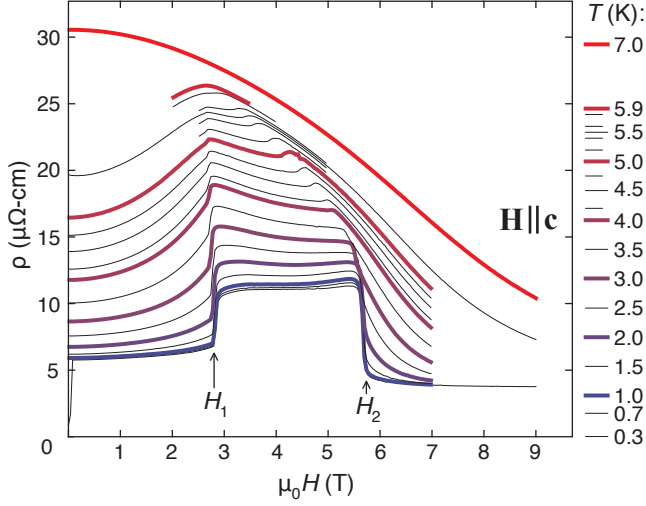


FIG. 3: In-plane resistivity of CeAuSb₂ against field, applied along the c axis. The plotted data are from increasing-field ramps.

Low-temperature measurements of the resistivity of CeAuSb₂ were done on two samples from the same growth batch, with cross sections $\approx 180 \times 130$ and $\approx 250 \times 150$ μm (the shorter dimension along the c axis). They were measured together in an adiabatic demagnetization refrigerator. Fig. 3 shows the resistivity of one sample against field at various fixed temperatures. At the lowest temperatures, ρ increases sharply at the first metamagnetic transition (at applied field H_1), and decreases sharply at the second (H_2). Elevated resistivity between H_1 and H_2 is also seen in CeNiGe₃ [4], YbNiSi₃ [8], and CeRh₂Si₂. [6]

Data from increasing-field and decreasing-field ramps are shown together in Fig. 4; magnet hysteresis is excluded by measuring the field with a Hall sensor placed near the sample. Hysteresis in the metamagnetic transition fields shows that the transitions are first-order. The magnitude of the hysteresis against temperature is shown in panel (b): it decreases steadily as the temperature is increased (proving that it is not an artefact of instrument hysteresis), disappearing within experimental resolution above ~ 5 K for the first and above ~ 3 K for the second transition.

Rounding of the transitions and remnant instrument hysteresis make it impossible to pinpoint the temperatures where the hysteresis ends. To locate the endpoints more precisely, we analysed the magnitudes of the resistivity jumps, $|\Delta\rho|$, determined by integrating the peaks in the derivative $d\rho/d(\mu_0 H)$ as illustrated in Fig. 5(a). Rounding introduces moderate systematic error, but by following the same procedure at each temperature random error is minimized. $|\Delta\rho|$ against T is shown in Fig. 5(b); the error bars are the estimated systematic error. Linear fits through the higher-temperature points

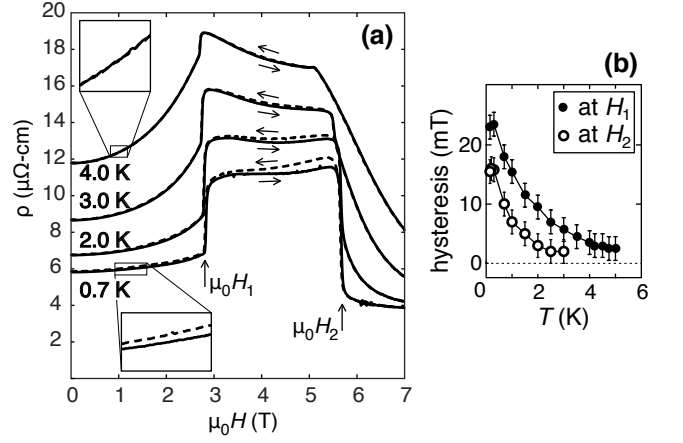


FIG. 4: (a) Data from increasing- and decreasing-field ramps, plotted together. (b) Difference in the transition fields between the increasing- and decreasing-field ramps, plotted against temperature. For all temperatures, the ramp rate was 0.1 T/min.

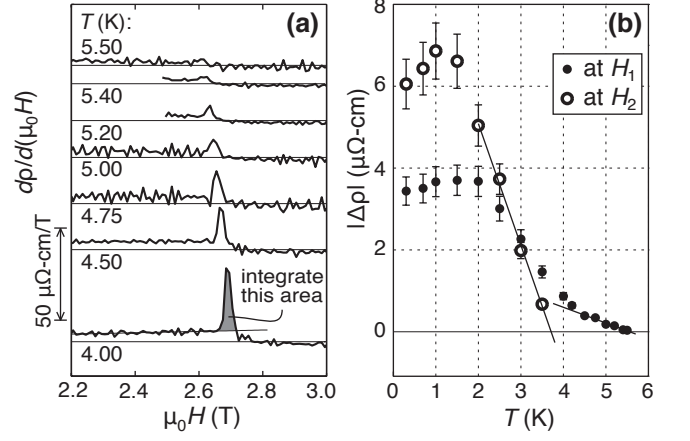


FIG. 5: (a) $d\rho/d(\mu_0 H)$ against $\mu_0 H$ at the first transition, at temperatures approaching the critical endpoint. On the bottom curve, the method for determining the resistivity jump $\Delta\rho$ is illustrated: a background is fit to the data to the left (right) of the peak for the first (second) metamagnetic transition, and the peak integrated. (b) $|\Delta\rho|$ against temperature.

locate the endpoints of the first and second transitions at 5.6 and 3.7 K, respectively.

In Fig. 4, hysteresis is apparent not only in the transition fields, but also in the magnitude of the resistivity across the magnetically ordered region: ρ is larger on decreasing- than increasing-field ramps. Hysteresis between H_1 and H_2 has been reported before; [2, 3] its origin is not resolved, although antiferromagnetic domain walls are a natural possibility. We add two further observations: (1) There is hysteresis below H_1 , as well as between H_1 and H_2 . (2) The magnitude of the hysteresis decreases approximately linearly as the temperature is increased, disappearing between 4 and

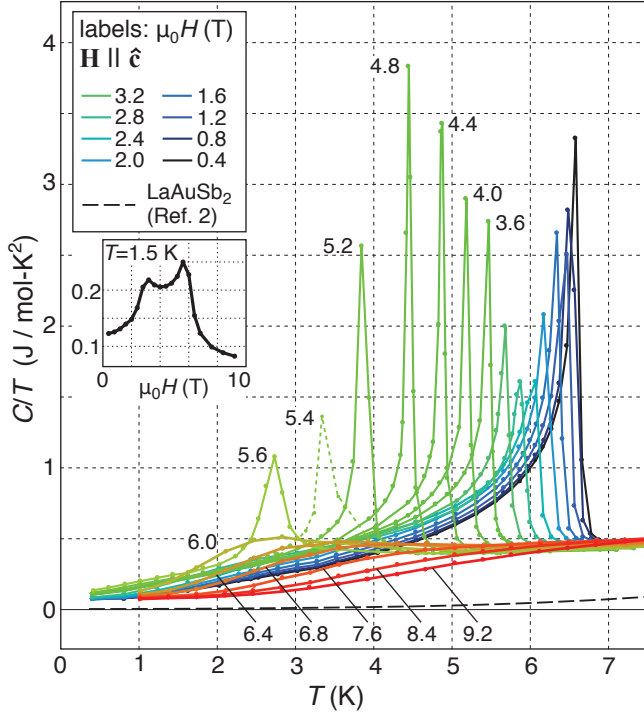


FIG. 6: Main panel: C/T of CeAuSb₂ at selected fields. Inset: C/T against field at $T = 1.5$ K.

5 K.

Results: specific heat capacity

The specific heat capacity C of a sample roughly 2 mm across and 0.1 mm thick, with mass 4.0 mg, was measured in a Quantum Design Physical Properties Measurement System. The relaxation time method was used: at each point the sample temperature was raised by 2%, then the relaxation time was measured.

C/T against temperature at selected magnetic fields is plotted in Fig. 6. C/T of LaAuSb₂, from Ref. [2], is also shown, as an estimate of the nonmagnetic contribution; up to at least ~ 7 K it is much smaller than C/T of CeAuSb₂. The dominant feature in the low-temperature heat capacity of CeAuSb₂ is the Néel transition. At low fields, the peak at T_N is relatively narrow. It is broader in the vicinity of the first critical endpoint, at 2.6 T and 5.6 K, and becomes very sharp as the field is increased towards the second critical endpoint, at 5.2 T and 3.7 K.

The inset in Fig. 6 shows C/T against field at $T = 1.5$ K. It is higher between H_1 and H_2 than on either side. This behavior has also been established for CeNiGe₃ [4], Ce(Ru_{0.92}Rh_{0.08})₂Si₂ [16], CeRh₂Si₂ [7], and (though less pronounced) Ce_{0.9}La_{0.1}Ru₂Si₂ [11].

C/T may be integrated from 0 K at each field to yield the entropy, S . To do so, an extrapolation to 0 K is required, though the data extend to low enough temper-

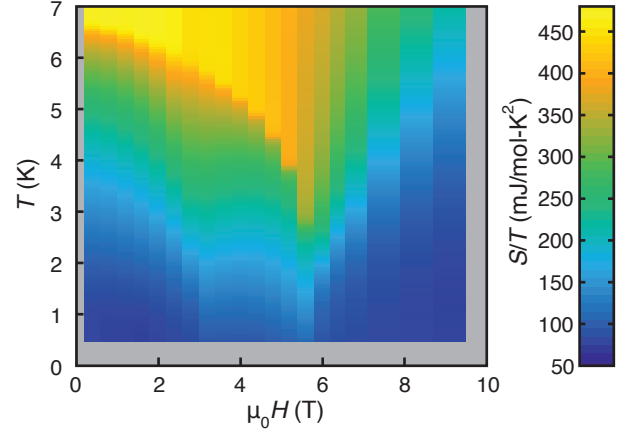


FIG. 7: Entropy over temperature of CeAuSb₂ against temperature and c -axis magnetic field.

ature that the precise form of the extrapolation is not critical. We take, at each field, a linear extrapolation from the lowest-temperature data point to 79.5 mJ/mol-K² at 0 K, which is an apparent base value in the data. A map of the resulting entropy, divided by temperature, is shown in Fig. 7. Below the Néel transition, the entropy is generally higher over the field range $H_1 < H < H_2$ than on either side.

At lower fields, S/T and C/T closely match above T_N : at $\mu_0 H = 0.4$ T and $T = 7$ K, S/T and C/T are 0.47 and 0.48 J/mol-K², respectively. In other words, the magnetic order maintains entropy balance with a Fermi-liquid-like, T -independent C/T . (Subtracting C/T of LaAuSb₂, as an estimate for the phonon contribution, makes little difference: S/T and C/T are respectively revised to 0.45 and 0.41 J/mol-K².) Entropy balance with a Fermi liquid suggests that the Ce 4f moments are fully incorporated into the Fermi liquid below some temperature that exceeds T_N , such that in the absence of magnetic order C/T would be T -independent down to 0 K. This behavior is in contrast to CeNiGe₃, YbNiSi₃, and Ce_{0.7}La_{0.3}Ru₂Si₂. Based on analysis of published data, [4, 8, 26] and taking reasonable extrapolations of C/T to 0 K, we find that in these compounds S/T at 7 K (above T_N for each) exceeds C/T by more than a factor of two. (Specifically, S/T and C/T at 7 K are respectively 0.65 and 0.30 J/mol-K² for CeNiGe₃, ≈ 0.63 and 0.27 J/mol-K² for YbNiSi₃, and ≈ 0.58 and 0.21 J/mol-K² for Ce_{0.7}La_{0.3}Ru₂Si₂.) In these compounds the 4f moments appear to give a quasi-independent contribution to S/T that is in addition to a Fermi liquid contribution: it appears that the moments are strongly disordered by $T \sim 7$ K, and so make a large contribution to the total entropy, but at 7 K the dominant contribution to C/T is from the Fermi liquid.

It is also notable that above T_N , C/T of CeAuSb₂ drops very quickly to its Fermi liquid value, whereas C/T

of each of CeNiGe_3 , YbNiSi_3 , and $\text{Ce}_{0.7}\text{La}_{0.3}\text{Ru}_2\text{Si}_2$ has a strong decaying tail that extends at least a few K above T_N . Such tails are common in local-moment systems, *e.g.* in PdCrO_2 , [27] and arise from gradual onset of short-range magnetic order above T_N . They provide further evidence that in these compounds the $4f$ moments and Fermi liquid are quasi-independent systems, while in CeAuSb_2 they are not.

At low fields, the entropy of CeAuSb_2 above T_N is a substantial fraction of $R \log 2$: at 0.4 T and 7 K, $S = 3.3 \text{ J/mol-K} = 0.57 R \log 2$. The $T > T_N$ entropy is gradually suppressed as the field is increased; it appears that the heavy fermion state is gradually suppressed through polarization of the Ce moments.

Results: high-field measurements

To probe the magnetic anisotropy, resistivity and torque magnetometry measurements up to 35 T were performed at the Laboratoire National des Champs Magnétiques Intenses in Grenoble, France. The samples were mounted on a rotatable platform, to vary the field angle. The transport sample was a bar with cross-sectional area $230 \times 90 \mu\text{m}$. The dimensions of the torque magnetometry sample were $\sim 250 \times 250 \times 50 \mu\text{m}$. Results are shown in Fig. 8.

Previously published measurements showed that T_N is almost independent of in-plane field up to 18 T. [2] Our measurements show similarly that the metamagnetic transition fields are remarkably unaffected by the presence of a strong in-plane field. In the figure, ρ is plotted against the c -axis field, $H_c = H \cos \theta$, with θ the angle between \mathbf{H} and the c axis. The form of $\rho(H_c)$ changes little as the in-plane field is increased, even to the point that \mathbf{H} is only a few degrees out of the plane.

The metamagnetic transitions are also apparent in the torque data. Plotted in the lower panel of Fig. 8 is the torque N divided by the in-plane field $H \sin \theta$: if the field-induced magnetization is pinned to the c axis, and is a function of H_c alone (*i.e.* independent of in-plane field), then the graph of $N/H \sin \theta$ against H_c will be independent of field angle. The data show that this is essentially the case for CeAuSb_2 up to $\theta \sim 70^\circ$, confirming that the magnetism of CeAuSb_2 is strongly easy-axis-type. As the field gets very close to the ab plane, the metamagnetic transitions move to lower H_c .

Phase diagram and Discussion

Fig. 9 shows the field-temperature phase diagram derived from the resistivity and specific heat data presented above. The first-order metamagnetic transition lines, and their critical endpoints, are indicated. The first metamagnetic line separates regions of magnetic order that may be designated the A and B phases. The line slopes leftward as T is raised, consistent with the observation that

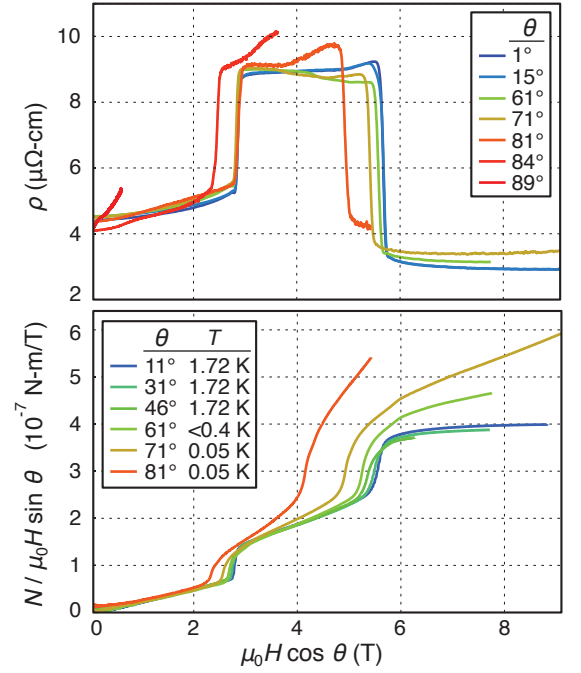


FIG. 8: Measurements of CeAuSb_2 in fields up to 35 T. θ is the angle between \mathbf{H} and the c axis. Upper panel: resistivity against c -axis field $\mu_0 H \cos(\theta)$. Lower panel: torque N , divided by the in-plane component of the field, against $\mu_0 H \cos(\theta)$. Measurements at 1.72 K were performed in St Andrews, and at lower temperatures in the high field laboratory in Grenoble.

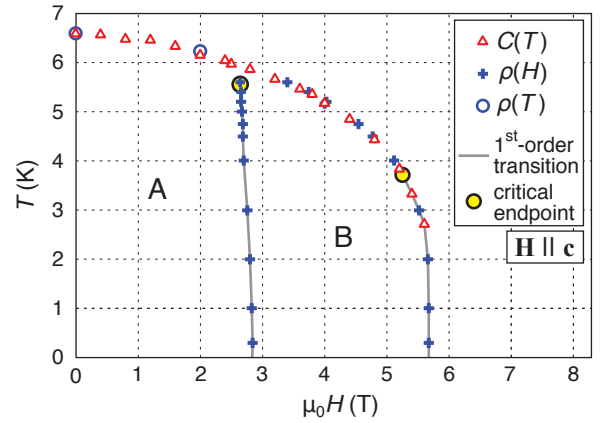


FIG. 9: Phase diagram of CeAuSb_2 , derived from measurements of ρ against H , ρ against T , and specific heat against T .

the B phase has higher entropy than the A phase. In contrast to a previous report, we do not find evidence for an intermediate phase along either metamagnetic line. [3]

The first critical endpoint, at a temperature of 5.6 K, appears to lie $\approx 0.4 \text{ K}$ below T_N at that field, although the present data cannot exclude with high confidence that it is not in fact on the Néel line. If it is indeed below

T_N , it would be interesting to determine whether the boundary between the A and B phases continues to T_N as a crossover or a second-order transition; the former implies adiabatic continuity between the two phases, and the latter an additional symmetry breaking.

Quantum criticality is a major theme in study of heavy-fermion systems, and in studies of criticality the locations of critical endpoints is vital knowledge. For example, many key properties of CeRu_2Si_2 are explainable by a missed quantum critical endpoint at $\mu_0 H \approx 7.6$ T. [28] At the famous field-driven antiferromagnetic quantum critical point of YbRh_2Si_2 , it is proposed that it is in fact close proximity of a metamagnetic critical endpoint and an antiferromagnetic QCP, rather than the antiferromagnetic QCP alone, that drives the observed divergences in the Sommerfeld coefficient and magnetic susceptibility. [29–31] The superconductivity of URhGe [32] and the anomalous phase in $\text{Sr}_3\text{Ru}_2\text{O}_7$ [33] both form around low-temperature metamagnetic critical endpoints.

In CeAuSb_2 , the second critical endpoint is at a temperature of 3.7 K. This is more than half the maximum T_N , so quantum critical scaling to $T \sim 0$ K is not expected. However it would be a very compelling experiment to track the endpoints with pressure, and to attempt to drive them to 0 K. The antiferromagnetic order of both CeRh_2Si_2 and CeNiGe_3 can be suppressed with pressure, with superconductivity appearing in a window of pressure around the antiferromagnetic QCP. [34, 35] It would be interesting to determine whether metamagnetic quantum criticality is also involved in this superconductivity. Regarding CeAuSb_2 , a published pressure study at $H = 0$ showed that pressure initially increases the temperature of the first resistivity shoulder and decreases T_N . [25]

As described above, entropy balance with a Fermi liquid suggests that Kondo coupling is important in CeAuSb_2 , incorporating the $4f$ moments into the Fermi liquid by some temperature that exceeds T_N ; strong Kondo coupling probably onsets at the temperature of the first resistivity shoulder, at ~ 12 K. Phenomenologically, CeAuSb_2 therefore appears to be intermediate to CeRu_2Si_2 , where Kondo coupling is strong enough that static magnetic order never emerges, and, *e.g.*, CeNiGe_3 and $\text{Ce}_{0.7}\text{La}_{0.3}\text{Ru}_2\text{Si}_2$, where the moments and conduction electrons appear to be quasi-decoupled at all temperatures.

We also note a strong similarity between the phenomenology of CeAuSb_2 and $\text{Sr}_3\text{Ru}_2\text{O}_7$, which was in fact the original motivation for this study of CeAuSb_2 : both show strongly enhanced resistivity over a finite window of field (in the case of $\text{Sr}_3\text{Ru}_2\text{O}_7$, between ≈ 7.9 and 8.1 T), bounded by first-order metamagnetic transitions, and over which the entropy is also higher. [33, 36] $\text{Sr}_3\text{Ru}_2\text{O}_7$ is very clearly an itinerant system, while in CeAuSb_2 the moments probably have strong local character below T_N . This similar behavior in spite of

this substantial difference suggests a deep link between the two systems.

Conclusion

In conclusion, we have produced a refined field-temperature phase diagram of CeAuSb_2 , and an entropy map spanning the region of magnetic order. We have also highlighted similarities between CeAuSb_2 and other compounds. The observed metamagnetic transitions were sufficiently sharp to resolve clear hysteresis, and to locate their critical endpoints, showing that CeAuSb_2 can now be grown with sufficiently low disorder to make it a useful reference material and target for further study.

We acknowledge useful discussion with Manuel Brando and Christoph Geibel. We thank Hanoh Lee for advice on crystal growth. We thank the EPSRC and the Max Planck Society for financial support. We also acknowledge the support of the LNCMI-CNRS, member of the European Magnetic Field Laboratory (EMFL). E.A.Y. acknowledges support from the Royal Society. P.C.C. was supported, in part, by the U.S. Department of Energy, Office of Basic Energy Science, Division of Materials Sciences and Engineering through the Ames Laboratory. Ames Laboratory is operated for the U.S. Department of Energy by Iowa State University under Contract No. DE-AC02-07CH11358. V.F. acknowledges support by the Deutsche Forschungsgemeinschaft through FOR 960. H.S. gratefully acknowledges fellowships from the Canon Foundation.

The raw data for the figures in this article can be found in Supplemental Material.

-
- [1] A. Thamizhavel, T. Takeuchi, T. Okubo, M. Yamada, R. Asai, S. Kirita, A. Galatanu, E. Yamamoto, T. Ebihara, Y. Inada, R. Settai, and Y. Onuki. Anisotropic electrical and magnetic properties of CeTSb_2 ($T=\text{Cu, au, and Ni}$) single crystals. *Phys. Rev. B* **68** 054427 (2003).
 - [2] L. Balicas, S. Nakatsuji, H. Lee, P. Schlottmann, T.P. Murphy, and Z. Fisk. Magnetic field-tuned quantum critical point in CeAuSb_2 . *Phys. Rev. B* **72** 064422 (2005).
 - [3] K.-A. Lorenzer, A.M. Strydom, A. Thamizhavel, and S. Paschen. Temperature-field phase diagram of quantum critical CeAuSb_2 . *Phys. Status Solidi B* **250** 464 (2013).
 - [4] E.D. Mun, S.L. Bud'ko, A. Kreyssig, and P.C. Canfield. Tuning low-temperature physical properties of CeNiGe_3 by magnetic field. *Phys. Rev. B* **82** 054424 (2010).
 - [5] A.P. Pikul, D. Kaczorowski, T. Plackowski, A. Czopnik, H. Michor, E. Bauer, G. Hilscher, P. Rogl, and Yu. Grin. Kondo behavior in antiferromagnetic CeNiGe_3 . *Phys. Rev. B* **67** 224417 (2003).
 - [6] W. Knafo, D. Aoki, D. Vignolles, B. Vignolle, Y. Klein, C. Jaudet, A. Villaume, C. Proust, and J. Flouquet. High-field metamagnetism in the antiferromagnet CeRh_2Si_2 . *Phys. Rev. B* **81** 094403 (2010).
 - [7] A. Palacio Morales, A. Pourret, G. Seyfarth, M.T.

- Suzuki, D. Braithwaite, G. Knebel, D. Aoki, and J. Flouquet. Fermi surface instabilities in CeRh_2Si_2 at high magnetic field and pressure. *Phys. Rev. B* **91** 245129 (2015).
- [8] S.L. Bud'ko, P.C. Canfield, M.A. Avila, and T. Takabatake. Magnetic-field tuning of the low-temperature state of YbNiSi_3 . *Phys. Rev. B* **75** 094433 (2007).
- [9] M.A. Avila, M. Sera, and T. Takabatake. YbNiSi_3 : An antiferromagnetic Kondo lattice with strong exchange interaction. *Phys. Rev. B* **70** 100409R (2004).
- [10] J.-M. Mignot, J.-L. Jacoud, L.-P. Regnault, J. Rossat-Mignod, P. Haen, P. Lejay, Ph. Boutrouille, B. Hennion, and D. Petitgrand. Neutron diffraction study of $(\text{Ce},\text{La})\text{Ru}_2\text{Si}_2$ alloys in an external field. *Physica B* **163** 611 (1990).
- [11] D. Aoki, C. Paulsen, T.D. Matsuda, L. Malone, G. Knebel, P. Haen, P. Lejay, R. Settai, Y. Ōnuki, and J. Flouquet. Pressure Evolution of the Magnetic Field Induced Ferromagnetic Fluctuations through the Pseudo-Metamagnetism of CeRu_2Si_2 . *J. Phys. Soc. Japan* **80** 053702 (2011).
- [12] Y. Shimizu, Y. Matsumoto, K. Aoki, N. Kimura, H. Aoki. Anomalous Transport Properties via the Competition between the RKKY Interaction and the Kondo Effect in $\text{Ce}_x\text{La}_{1-x}\text{Ru}_2\text{Si}_2$. *J. Phys. Soc. Japan* **81** 044707 (2012).
- [13] J.M. Mignot, L.P. Regnault, J.L. Jacoud, J. Rossat-Mignod, P. Haen, and P. Lejay. Incommensurabilities and metamagnetism in the heavy-fermion alloys $(\text{Ce}_{0.8}\text{La}_{0.1})\text{Ru}_2\text{Si}_2$ and $\text{CeRu}_2(\text{Si}_{0.9}\text{Ge}_{0.1})_2$. *Physica B* **171** 357 (1991).
- [14] M. Sugi, Y. Matsumoto, N. Kimura, T. Komatsubara, H. Aoki, T. Terashima, and S. Uji. Fermi Surface Properties of $\text{CeRu}_2(\text{Si}_{1-x}\text{Ge}_x)_2$ in Magnetic Fields above the Metamagnetic Transitions. *Phys. Rev. Lett.* **101** 056401 (2008).
- [15] C. Sekine, T. Sakakibara, H. Amitsuka, Y. Miyako, and T. Goto. Magnetic Properties and Phase Diagram of $\text{Ce}(\text{Ru}_{1-x}\text{Rh}_x)_2\text{Si}_2$ ($0 \leq x < 0.5$). *J. Phys. Soc. Japan* **61** 4536 (1992).
- [16] D. Aoki, C. Paulsen, H. Kotegawa, F. Hardy, C. Meingast, P. Haen, M. Boukahil, W. Knafo, E. Ressouche, S. Raymond, and J. Flouquet. Decoupling between Field-Instabilities of Antiferromagnetism and Pseudo-Metamagnetism in Rh-Doped CeRu_2Si_2 Kondo Lattice. *J. Phys. Soc. Japan* **81** 034711 (2012).
- [17] R. Settai, A. Misawa, S. Araki, M. Kosaki, K. Sugiyama, T. Takeuchi, K. Kindo, Y. Haga, E. Yamamoto, and Y. Ōnuki. Single Crystal Growth and Magnetic Properties of CeRh_2Si_2 . *J. Phys. Soc. Japan* **66** 2260 (1997).
- [18] P. Haen, J. Flouquet, F. Lapierre, P. Lejay, and G. Remenyi. Metamagnetic-like Transition in CeRu_2Si_2 ? *J. Low Temp. Phys.* **67** 391 (1987).
- [19] S. Raymond, L.P. Regnault, S. Kambe, J. Flouquet., and P. Lejay. Switching of the magnetic interactions from antiferromagnetic to ferromagnetic in the heavy-fermion compound CeRu_2Si_2 under high magnetic field. *J. Phys.: Condensed Matter* **10** 2363 (1998).
- [20] A. Amato, D. Jaccard, J. Sierro, P. Haen, P. Lejay, and J. Flouquet. Transport Properties under Magnetic Fields of the Heavy Fermion System CeRu_2Si_2 and Related Compounds $(\text{Ce},\text{La})\text{Ru}_2\text{Si}_2$. *J. Low Temp. Phys.* **77** 195 (1989).
- [21] W. Knafo, S. Raymond, P. Lejay, and J. Flouquet. Antiferromagnetic criticality at a heavy-fermion quantum phase transition. *Nat. Phys.* **5** 753 (2009).
- [22] P. Haen, F. Lapierre, J. Voiron, J. Flouquet. Vanishing of magnetic order in $\text{Ce}_{0.8}\text{La}_{0.2}\text{Ru}_2\text{Si}_2$ under pressure. *J. Phys. Soc. Japan* **65** (Suppl. B) 27 (1996).
- [23] P.C. Canfield and Z. Fisk. Growth of single-crystals from metallic fluxes. *Philosophical Magazine B* **65** 1117 (1992).
- [24] P.C. Canfield and I.R. Fisher. High-temperature solution growth of intermetallic single crystals and quasicrystals. *J. Crystal Growth* **225** 155 (2001).
- [25] S. Seo, V.A. Sidorov, H. Lee, D. Jang, Z. Fisk, J.D. Thompson, and T. Park. Pressure effects on the heavy-fermion antiferromagnet CeAuSb_2 . *Phys. Rev. B* **85** 205145 (2012).
- [26] M.J. Besnus, P. Lehmann, and A. Meyer. Heat capacity study of the $(\text{La}-\text{Ce})\text{Ru}_2\text{Si}_2$ and $(\text{Ce}-\text{Y})\text{Ru}_2\text{Si}_2$ Kondo systems. *Journal of Magnetism and Magnetic Materials* **63 & 64** 323 (1987).
- [27] H. Takatsu, H. Yoshizawa, S. Yonezawa, Y. Maeno. Critical behavior of the metallic triangular-lattice Heisenberg antiferromagnet PdCrO_2 . *Phys. Rev. B* **79** 104424 (2009).
- [28] F. Weickert, M. Brando, F. Steglich, P. Gegenwart, and M. Garst. Universal signatures of the metamagnetic quantum critical endpoint: Application to CeRu_2Si_2 . *Phys. Rev. B* **81** 134438 (2010).
- [29] T. Misawa, Y. Yamaji, and M. Imada. YbRh_2Si_2 : Quantum Tricritical Behavior in Itinerant Electron System. *J. Phys. Soc. Japan* **77** 093712 (2008).
- [30] A. Hackl and M. Vojta. Zeeman-Driven Lifshitz Transition: A Model for the Experimentally Observed Fermi-Surface Reconstruction in YbRh_2Si_2 . *Phys. Rev. Lett.* **106** 137002 (2011).
- [31] P. Gegenwart, J. Custers, Y. Tokiwa, C. Geibel, and F. Steglich. Ferromagnetic quantum critical fluctuations in $\text{YbRh}_2(\text{Si}_{0.95}\text{Ge}_{0.05})_2$. *Phys. Rev. Lett.* **94** 076402 (2005).
- [32] E.A. Yelland, J.M. Barracough, W. Wang, K.V. Kamenev and A.D. Huxley. High-field superconductivity at an electronic topological transition in URhGe . *Nat. Physics* **7** 890 (2011).
- [33] S.A. Grigera, P. Gegenwart, R.A. Borzi, F. Weickert, A.J. Schofield, R.S. Perry, T. Tayama, T. Sakakibara, Y. Maeno, A.G. Green, A.P. Mackenzie. Disorder-Sensitive Phase Formation Linked to Metamagnetic Quantum Criticality. *Science* **306** 1154 (2004).
- [34] H. Kotegawa, K. Takeda, T. Miyoshi, S. Fukushima, H. Hidaka, T.C. Kobayashi, T. Akazawa, Y. Ohishi, M. Nakashima, A. Thamizhavel, R. Settai, and Y. Ōnuki. Pressure-induced superconductivity emerging from antiferromagnetic phase in CeNiGe_3 . *J. Phys. Soc. Japan* **75** 044713 (2006).
- [35] S. Araki, M. Nakashima, R. Settai, T.C. Kobayashi, Y. Ōnuki. Pressure-induced superconductivity in an antiferromagnet CeRh_2Si_2 . *J. Phys.: Condensed Matter* **14** L377 (2002).
- [36] A.W. Rost, R.S. Perry, J.-F. Mercure, A.P. Mackenzie, S.A. Grigera. Entropy Landscape of Phase Formation Associated with Quantum Criticality in $\text{Sr}_3\text{Ru}_2\text{O}_7$. *Science* **325** 1360 (2009).